

Three-dimensional valve-based controllable PDMS nozzle for dynamic modulation of droplet generation

Bo Cai¹ · Rongxiang He² · Xiaolei Yu¹ · Lang Rao¹ · Zhaobo He¹ · Qinqin Huang¹ · Wei Liu¹ · Shishang Guo¹ · Xing-Zhong Zhao¹

Received: 6 December 2015 / Accepted: 20 February 2016 / Published online: 19 March 2016
© Springer-Verlag Berlin Heidelberg 2016

Abstract In this work, we developed a shape-controllable nozzle inside a multilayer PDMS microchip. The nozzle was able to control the shape of the fluid channel in three dimensions. All the four walls of the fluid channel were comprised of pneumatic PDMS membrane valves, and their deformation was controlled by air pressure. As both the limitation of the fluid flux and the shape of the fluid channel were adjustable spatially in three dimensions, this valve-based nozzle generated droplets with less response time and in a more effectively controlled manner comparing to conventional droplet devices. It could also function as a microinjector to modulate the compositions of droplets precisely and continuously. In addition, the nozzle was able to form a specific shape to generate core-shell particles.

Keywords Soft nozzle · Pneumatic valves · Droplets · Adjustable particle generation

1 Introduction

Droplet microfluidics has provided countless novel methods for chemical and biological researches (Christopher and Anna 2007; Kelly et al. 2007; Rosenfeld et al. 2014; Teh et al. 2008; Yang et al. 2010). It has many unique advantages, such as compartmentalization, high surface/volume ratio, quantification, monodispersity and high throughput (Chiu et al. 2009; Theberge et al. 2010). These nano- to pico-liter-scale droplets can function as individual nano-laboratories to facilitate material synthesis (Puigmarti-Luis 2014; Yang et al. 2012; Zhao et al. 2015), trace detection (Chokkalingam et al. 2013; Guo et al. 2011, 2012a), cell encapsulation and culture (Agarwal et al. 2013; Cai et al. 2014; Velasco et al. 2012), single-cell analysis (Guo et al. 2012b; Hazel et al. 2013; Jarosz et al. 2014), drug delivery and evaluation (Garrait et al. 2014; Yu et al. 2010) and so on.

Originally, in microfluidic chips, droplets are generally formed in passive hydrodynamic formats using flow-focusing, T-junction or coaxial structures (Christopher and Anna 2007; Teh et al. 2008). The elaborately designed microchannels help to generate varied droplets that have specific structures for unique functions in a high-throughput way (Datta et al. 2014; Ji et al. 2011; Shang et al. 2014). To improve the maneuverability of the droplet generation in microchannels, active formats that mainly employ actuators to regulate the fluid flow are developed. Many techniques, such as mechanical, electric, thermal and acoustic methods, have been employed for droplet manipulations (Chong et al. 2016; Collins et al. 2015). Among them, the pneumatic valve-based droplet-on-demand (DOD) systems are representative (Guo et al. 2010; Wang et al. 2009; Zeng et al. 2009), which can benefit on-chip sample treatments in a more sensitive manner (Chong et al. 2016). There are

Electronic supplementary material The online version of this article (doi:10.1007/s10404-016-1725-2) contains supplementary material, which is available to authorized users.

✉ Xing-Zhong Zhao
xzzhao@whu.edu.cn

¹ Key Laboratory of Artificial Micro- and Nano-structures of Ministry of Education, School of Physics and Technology, Wuhan University, Wuhan, China

² Institute for Interdisciplinary Research & Key Laboratory of Optoelectronic Chemical Materials and Devices, Ministry of Education, Jiangnan University, Wuhan, China

mainly two kinds of pneumatic valves. One is single-layer membrane valves (SLMVs) that integrate the control and fluid channels into a single polydimethylsiloxane (PDMS) layer. The other is multilayer membrane valves (MLMVs), which utilize vertical deflection of an elastic PDMS membrane to modulate the flow in the fluid channel (Lee et al. 2009; Ochs and Abate 2015). Through multiple combinations of valves and pumps, the volume, frequency and patterns of the generated droplets can be effectively controlled in a fast and precise manner.

However, these droplet systems face some challenges. Although the passive droplet microfluidics is high-throughput, it is greatly limited when dealing with situations that need to manipulate droplets flexibly (Guo et al. 2010; Hsieh et al. 2009), e.g., those multi-step bioassays which need to adjust reagents in droplets at different time (Abate et al. 2010; Chen et al. 2013). Moreover, the passive formats, which regulate droplet manipulations using fluid-driven apparatus, can hardly change fluid conditions fast or flexibly enough. Pneumatic DOD systems facilitate versatile manipulations of droplets. Nevertheless, they still have some limitations. As the pneumatic valves inserted in these DOD system could only control channel walls in one dimension (horizontal as SLMVs or vertical as MLMVs), they lack fast response to regulate droplet formation/concentration effectively. And the existence of dead volume when dealing with the rectangular

fluid channels hinders their regulation performance of the fluid inside (Lai et al. 2008; Oh et al. 2015; Unger et al. 2000). For SLMVs, the existence of dead volumes will lead to uncontrollable leakage when the valves are closed. Although MLMVs with rounded channels can provide favorable on-off performance, specialized photoresist and techniques are needed.

Herein, we developed a shape-controllable nozzle inside a multilayer PDMS chip by mounting pneumatic valves around the fluid channel in three dimensions. This design enabled fast, precise and versatile generation and modulation of microscale droplets (Fig. 1). Utilizing multilayer soft lithography (Unger et al. 2000) novelly, a microchannel section with four deformable walls was formed. These four membrane valves around the fluid channel were assembled to work as a 3D controllable nozzle. The addition of a pair of vertical valves besides the pair of horizontal valves raises the maneuverability of the deformation of the fluid channels. When different pressures are applied into the air chambers, the four membrane walls deformed to different extents, thus causing the fluid channel to open, form nozzle or close. After integrated with droplet generation structures, this 3D adjustable valve-based nozzle could regulate the formation of different droplets. Also, it could function as a microinjector to control the compositions of droplets effectively. Due to the flexibility of the movement of the four channel walls, this structure could form a unique nozzle shape to generate

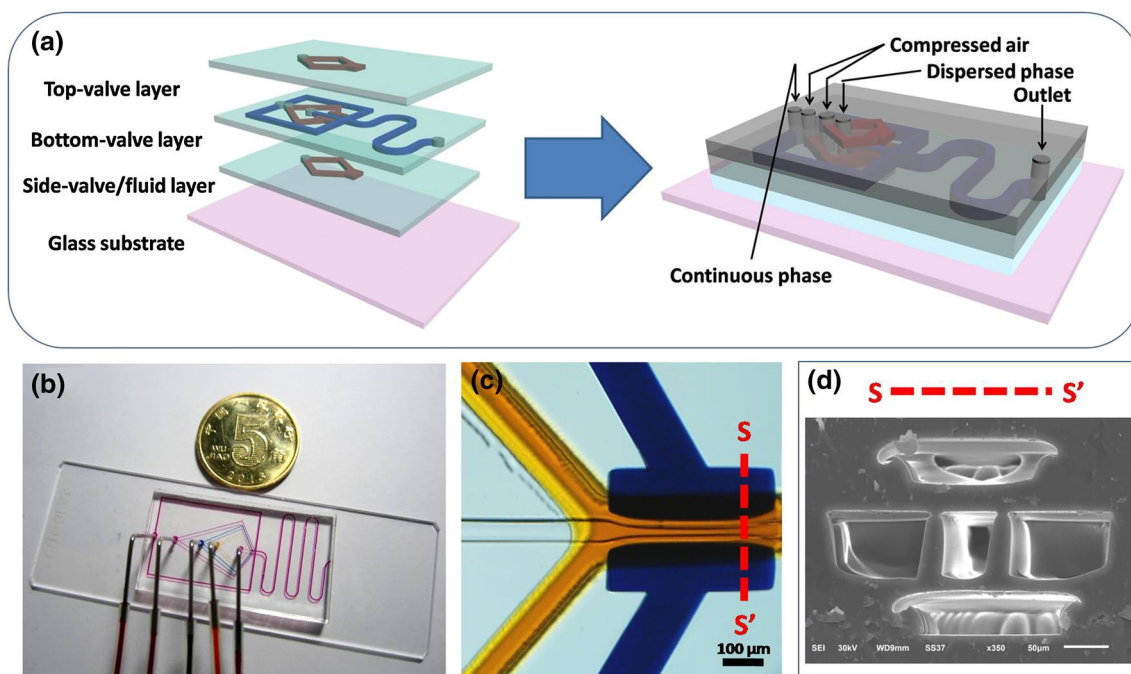


Fig. 1 **a** Schematic of the 3D valve-based controllable nozzle which was integrated in a droplet generation microchip. **b** A photograph of a droplet generation microchip integrating the 3D valve-based con-

trollable nozzle. **c** Bright-field image and **d** corresponding cross-sectional scanning electron microscope (SEM) image of the 3D valve-based controllable nozzle

core-shell particles, providing a facile and controllable strategy for multi-functional particle synthesis.

2 Experiment

2.1 Chip fabrication

To fabricate this 3D valve-based nozzle, at first, a mold of top and bottom valve (Mold 1) was made with the height of 10 μm , while the other mold of side valves and fluid channels (Mold 2) was made with the height of 50 μm . Both molds were fabricated using SU-8 photoresist (MicroChem, USA) through conventional photolithography technique. Then a 5-mm-thick PDMS layer (with *A/B* ratio of 10:1, RTV615, GE Toshiba Silicone Corp., USA) of top valve was casted from Mold 1 [Fig. 2a(1)]. Subsequently, uncured PDMS (with *A/B* ratio of 20:1) was spin-coated onto Mold 2 (at 750 rpm) and baked for 15 min to be precisely aligned and stamped by the top-valve layer. These two layers of PDMS were baked for 30 min (at 80 $^{\circ}\text{C}$) to irreversibly bond to each other [Fig. 2a(2)]. And then, another PDMS spin-coating procedure was implemented at 1200 rpm with *A/B* ratio of 10:1 on Mold 1. After a 5-min bake at 80 $^{\circ}\text{C}$, the as-prepared two PDMS layers and the bottom-valve layer were carefully aligned and then baked again for the bonding [Fig. 2a(3)]. Finally, when the three-layer PDMS bulk was peeled off and the holes were punched, it was bonded to a glass substrate with the oxygen plasma treatment [Fig. 2a(4)]. The newly fabricated chips mounted with the 3D valve-based nozzles were then baked at 120 $^{\circ}\text{C}$ for another 12 h to regain hydrophobicity for better droplet generation performance (Rao et al. 2015).

2.2 Chip design for basic flow-focusing structure and multiplex flow-focusing structure (the microinjector)

In this paper, we mainly mounted such 3D valve-based nozzle onto two kinds of droplet generation structures (the basic flow-focusing structure as shown in Fig. 2b, d and the multiplex flow-focusing structure as shown in Fig. 2c, e). We utilized these two designs to demonstrate the advantages of the nozzle for fast and versatile droplet formation regulation, as well as to show its unique application in the controllable formation of core-shell particles in microscale.

In both structures, for the 3D valve-based nozzle part, its side valves were comprised of two square chambers whose length and width were 400 and 100 μm , respectively (shown by blue dye in Fig. 2d, e), and they were supported by a 100- μm -wide microchannel (the red line in Fig. 2b, c) which provided compressed air. The distance between side valves and the fluid channel was 25 μm . The top and

bottom valves were 500 μm long and 130 μm wide (shown by yellow dye in Fig. 2d, e), and they were supported by a 50- μm -wide microchannel (the green dash line in Fig. 2b, c) which provided compressed air.

For the fluid microchannels, in the basic flow-focusing structure, channels for continuous phase (the yellow line in Fig. 2b) were all 100 μm in width, and the dispersed fluid channel (the blue line in Fig. 2b) was 50 μm wide. In the multiplex flow-focusing structure, channels for continuous phase (the yellow line in Fig. 2c) were 200 μm in width. The dispersed fluid channel in the middle (the blue line in Fig. 2c) was just 50 μm wide. And in order to form a microinjector to precisely control the contents of the droplets, we designed two more 100- μm -wide fluid channels for another kind of dispersed phase (the gray line in Fig. 2c). This structure was also used to generate core-shell microparticles when the 3D valve-based nozzle formed a specific structure. All the fluid channels for both structures were about 50 μm in height.

2.3 3D valve-based nozzle manipulations and the fluid regulation

The pneumatic valves of our 3D nozzle integrated in the microchips were filled with water and actuated by the compressed air that was generated by an air compressor (Linkstrong-tech Corp., China). The functions of the gas circuit were implemented via electronic solenoid valves (Series S070, SMC, Japan). These valves were under the control of a data acquisition module (USB-4750, Advantech, USA), which was driven by a custom-built program written using LABVIEW 8.6 software (National Instruments, USA).

In our experiments, the mineral oil (Beiya Medical Oil Corp., China) with 2 % span-80 (the surfactant to avoid droplet coalescence, National Medicines Corp., China) was adopted as the continuous phase. For the basic flow-focusing structure, we used the deionized water (DI water, purified by Millipore Direct-Q3 water purification system, Millipore, USA) as the dispersed phase. In the multiplex flow-focusing structure, the blue ink (BI) was used as another dispersed phase to demonstrate the precise and controllable modulation of contents in droplets. And to generate core-shell particles, we used 1 % sodium alginate (National Medicines Corp., China) doped with Fe_3O_4 nanoparticles [synthesized using hydrothermal method previously reported (Yu et al. 2013)] as the visible core phase and 1.5 % pure sodium alginate as the shell phase. 1 % calcium acetate (National Medicines Corp., China) was added into the continuous phase as the cross-linking agent for sodium alginate to obtain solid core-shell beads. All the fluids in our experiments were driven by syringe pumps (TS2-60, Longer Precision Pump Corp., China).

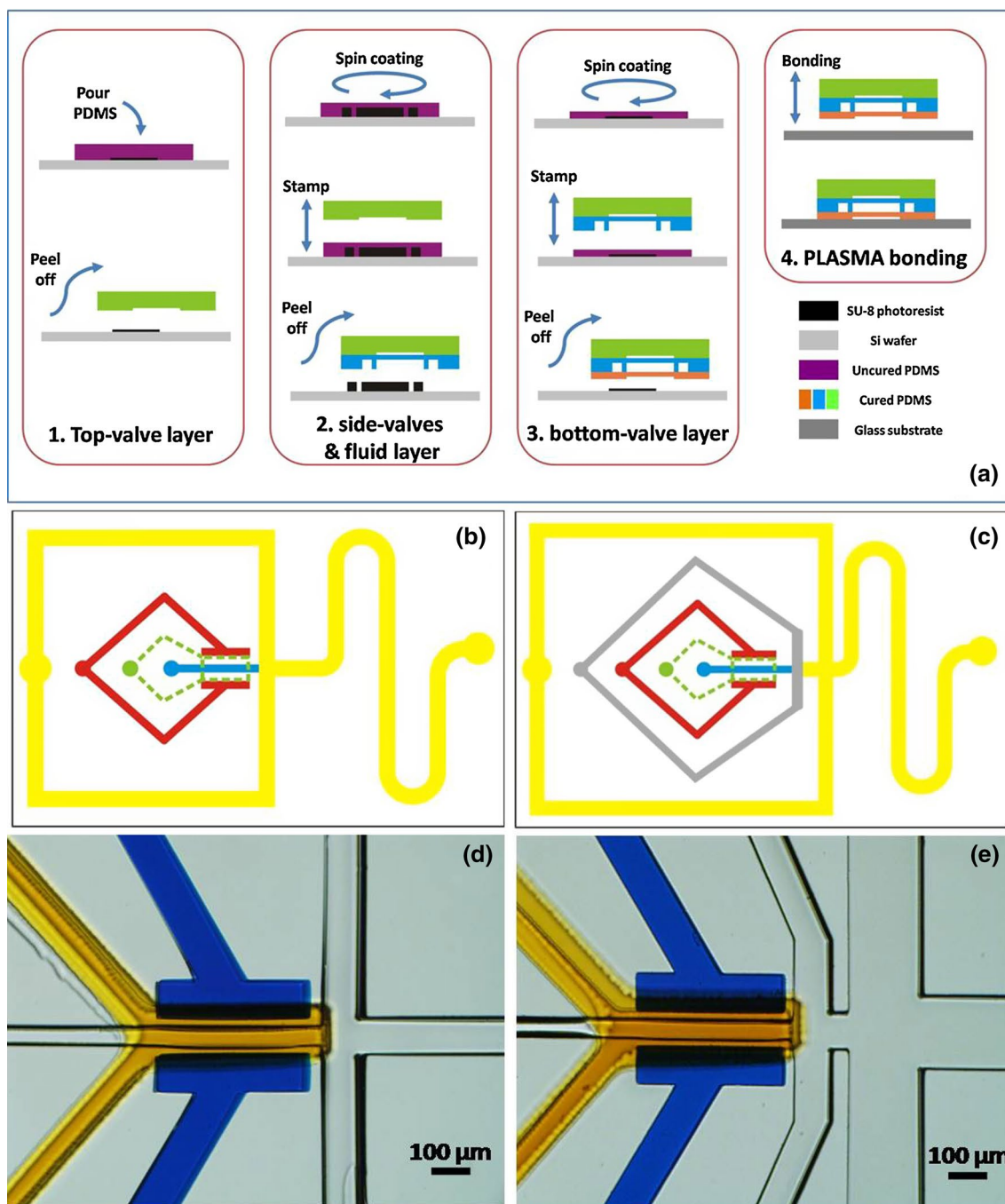


Fig. 2 **a** Workflow diagram showing the fabrication procedure of the 3D valve-based controllable nozzle. **b, d** Schematic and bright-field image of the 3D valve-based nozzle which was mounted on the basic flow-focusing orifice for precise droplet generation regulation. **c, e**

Schematic and bright-field image of the 3D valve-based nozzle which was mounted on the multiplex flow-focusing structure as a microinjector (color figure online)

3 Results and discussion

To demonstrate the advantages of our 3D valve-based controllable nozzle in droplet formation regulation, we compared the droplet regulation performance of this nozzle to other strategies (i.e., hydrodynamic flow-focusing method and valve-based DOD systems using SLMVs and MLMVs).

3.1 3D valve-based nozzle regulating droplet formation for basic flow-focusing structure

As shown in Fig. 3a, at first, we mounted our 3D valve-based nozzle on the dispersed fluid channel of a basic flow-focusing structure to demonstrate its ability for fast and precise generation of microscale droplets. Some literatures

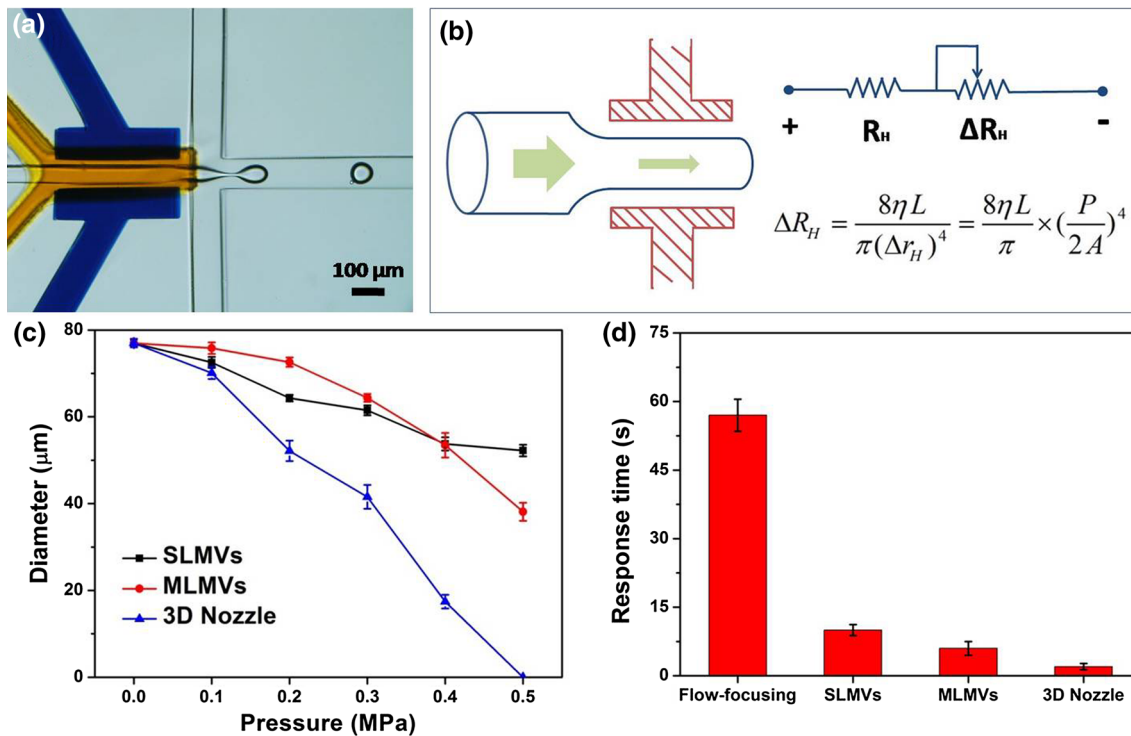


Fig. 3 **a** 3D valve-based nozzle regulating droplet formation for basic flow-focusing structure. **b** The hydraulic resistance of the microchannel mediated by the 3D valve-based nozzle. **c** The relation-

ship between droplet diameter and the pressure used to control different kinds of valves. **d** The response time of different kinds of valve structures for droplet diameter regulation

reported a regime design that put two pneumatic valves symmetrically just downstream the flow-focusing orifice to regulate both the continuous and dispersed phase simultaneously (Abate et al. 2009; Angile et al. 2014). Differently, our nozzle just controlled the shape of dispersed fluid channel and acted like a “rheostat” to change the hydraulic resistance continuously (Oh et al. 2012). It indeed helped to regulate the generation of droplets in a controllable manner (Fig. 3b). The hydraulic resistance of the dispersed fluid channel in our design could be expressed as:

$$R = R_H + \Delta R_H$$

Here, R_H was the hydraulic resistance of the dispersed fluid channel before the nozzle, while ΔR_H represented the hydraulic resistance of the dispersed fluid channel controlled by the 3D valve-based nozzle. Because the channel was mainly rectangular, we had:

$$\Delta R_H = \frac{8\mu L}{\pi(\Delta r_H)^4} = \frac{8\mu L}{\pi} \times \left(\frac{P}{2A}\right)^4$$

where μ was the viscosity of the dispersed phase and L was the length of the channel that was regulated by the nozzle. The hydraulic radius of the channel Δr_H was a geometric constant and defined as $\Delta r_H = 2A/P$, where A was the cross-sectional area of the channel and P was the wetted

perimeter. Both of these parameters were evidently controlled by the nozzle. Therefore, the pressure of the compressed air precisely regulated Δr_H . Although the flow rate of the dispersed phase Q_d was fixed by the syringe pump, the practical flow rate of the dispersed phase Q_{in} in the microchannel was just a fraction of the set value of the syringe pump, i.e., $Q_{in} = \alpha Q_d$, where α typically depended on the hydraulic resistance R of the whole dispersed fluid channel (Liu and Yobas 2015). As previously reported, the diameter of droplets depended on the flow rate ratio of both dispersed and continuous phase (Anna et al. 2003; Baroud et al. 2010; Fu et al. 2012), thus we ensured that the regulation of our 3D valve-based nozzle on the flux of the dispersed fluid controlled the generation of the microscale droplets.

Indeed, comparing to other three regulation methods in our experiments, the 3D valve-based nozzle showed higher sensitivity and effectiveness when modulating the droplet generation procedure. As shown in Fig. 3c, through adjusting the input pressure of the compressed air, this 3D nozzle was able to modulate the diameter of the generated droplets (the flow rate of continuous mineral oil phase and dispersed deionized water phase were 147 and 21 $\mu\text{L/h}$, respectively). Although SLMVs or MLMVs also acted as actuators to adjust the droplet diameters, it was noticeable that their ability to control the droplet formation was quite

limited (around 40–80 μm), which would not satisfy the demand that required a wide range of variation of droplet size. In addition, as the pressure of the compressed air increased (higher than 0.3 MPa), the droplet size was not effectively reduced adopting SLMVs or MLMVs. It indicated that, within the threshold of the pressure that PDMS valves could afford (a little higher than 0.5 MPa in our experiments), SLMVs or MLMVs could not seal the rectangular channel effectively due to the existence of dead volume. Nevertheless, the 3D valve-based nozzle was able to cut off the flow of dispersed phase in the flow-focusing orifice completely. Indeed, it has no dead volume because of the deformation ability of all the four channel walls. This property endowed the 3D valve-based nozzle with more flexibility in droplet formation and downstream manipulations for droplet-based assays.

Also, our 3D valve-based nozzle showed faster response during fluid regulation (Fig. 3d) among the methods we tested. Here, we defined the “response time” as the time consumed for the droplets to change from the original size to the appointed one. The droplet size was measured by analyzing the image sequence acquired by a CCD camera (DP72, Olympus, Japan). Basic flow-focusing droplet formation was a passive hydrodynamic format and mainly implemented using syringe pumps. So the adjustment of the droplet size was at slow response (about 1 min), due to the delay of the apparatus and flow resistance from connecting tubes and microchannels. This was obviously detrimental for some chemical or biological reactions that required fast modulation of reagent concentration or continuous variation of injected materials. Pneumatic DOD systems using either SLMVs or MLMVs effectively reduced the response time. However, as they could only control channel walls in one dimension, these DOD systems still needed about 10 s to regulate droplet formation effectively. For the 3D valve-based nozzle, all the four channel walls were controlled by the compressed air at the same time. This design increased the deformation of the soft PDMS channel compared to other DOD systems when using the same pressure, thus it acted faster and undoubtedly facilitated the droplet-based reactions that needed fast regulation.

3.2 3D valve-based nozzle as a microinjector for regulation of composition concentration in droplets

After integrated with a multiplex flow-focusing structure, the 3D valve-based nozzle functioned as a controllable injector for precise modulation of droplet composition (Fig. 4a). As a proof of concept showing its application for droplet-based mixture and chemical reactions, we injected blue ink (BI) into the deionized water (DI) and

formed hybrid droplets whose BI concentration could be detected precisely through optic analysis. At first, the BI was injected into the DI directly at a flow rate ratio of 1:2, and their mixture formed droplets at the subsequent flow-focusing orifice with BI concentration of about 34 %. Through adjusting the pressure of compressed air that actuated the 3D valve-based nozzle, we could effectively modulate the flow of BI. And by analyzing the absorption percentage of the light using Image Pro Plus software, the concentration of the well-mixed droplet was given as:

$$\eta = \frac{\ln I_b - \ln I_m}{\ln I_b - \ln I_o}$$

where I_b , I_m and I_o were the average optic intensity of the background signal, the modulated mixed droplet and original generated droplet, respectively (Guo et al. 2010). Firstly, we investigated the response time of our nozzle to ensure its fast variation of the contents of generated droplets. Here, we defined the “response time” as the time that was needed for the device to change the concentration of droplets from the origin to the appointed one. The result is shown in Fig. 4b, which was similar to the size adjustment demonstrated in Fig. 3d. Figure 4c shows that SLMVs, MLMVs and our 3D valve-based nozzle had similar modulation performance like their regulation of the droplet size. The 3D valve-based nozzle, as a facile controllable microinjector, adjusted the concentration of the additive precisely. Because this microinjector contained no dead volume, the 3D valve-based nozzle completely stopped the injection of one of the reagents, and thus helped to control the reactions in the droplets totally. To validate the accuracy of concentration modulation of our nozzle and the corresponding optic detection method, we implemented droplet formation with different BI concentration and compared the results to theoretical calculations (Fig. 4d). We adjusted the flow rates of BI and DI phase to obtain certain ratio to form droplets. The concentration calculation of the generated droplets was described as:

$$\eta = \frac{V_{\text{BI}}}{V_{\text{DI}} + V_{\text{BI}}} = \frac{f_{\text{BI}} \times t}{f_{\text{DI}} \times t + f_{\text{BI}} \times t} = \frac{f_{\text{BI}}}{f_{\text{DI}} + f_{\text{BI}}}$$

where V_{BI} and V_{DI} represented the volume of BI and DI phase injected into the droplets, while f_{DI} and f_{BI} represented the flow rate of BI and DI phase, respectively. It was obvious that our detection stratagem fitted the calculation precisely. After integrated with chemical or biological luminescence/fluorescence methods, our 3D valve-based nozzle would have great potentials for precise droplet-based reaction regulation.

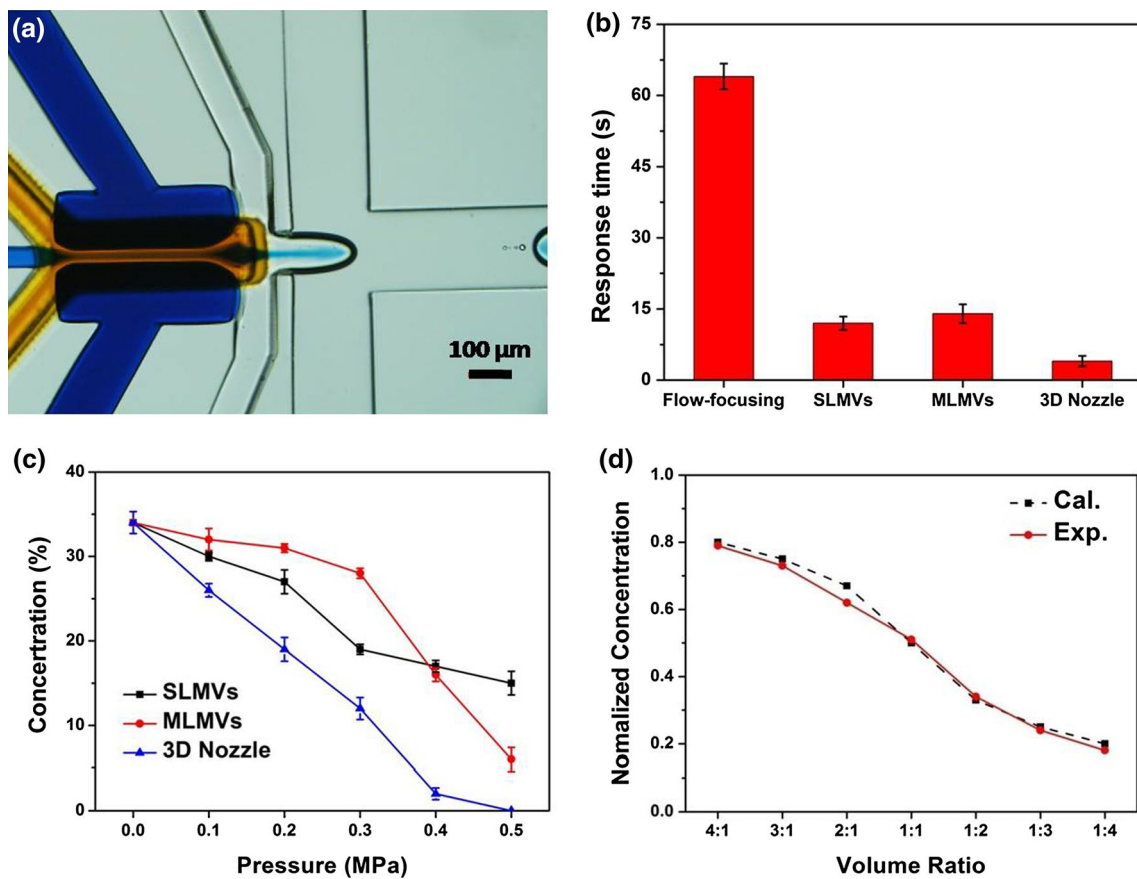


Fig. 4 **a** 3D valve-based nozzle as a microinjector for regulation of composition concentration in droplets. **b** The response time of different kinds of valve structures for concentration regulation in droplets. **c** The relationship between the concentration of BI in droplets and the

pressure used to control different kinds of valves. **d** BI concentration in droplets measured by image analysis versus the corresponding theoretical calculations

3.3 Core-shell microparticle formation using the 3D valve-based nozzle

By properly adjusting the pressure of the compressed air, core-shell particles were generated by the 3D valve-based nozzle (Fig. 5a, b). We used 1 % sodium alginate doped with Fe₃O₄ nanoparticles as the visible core phase (the flow rate was set at 21 μL/h) and 1.5 % pure sodium alginate as the shell phase (with flow rate of 14 μL/h). The mineral oil with 2 % span-80 and 1 % calcium acetate was used as the continuous phase, and its flow rate was set at 138 μL/h. By applying appropriate pressure of the compressed air, those pneumatic valves around the fluid channel pressed the four walls to form a nozzle for the core phase (Fig. 5c). After carefully adjusting the flow rates of the core and shell phase, the 3D valve-based nozzle forced the core phase jetting into the shell phase and then the two phases were sheared off into droplets by the continuous phase. Then the core phase was encapsulated into the shell phase to form core-shell structure. In the downstream channel, the Ca²⁺ cation provided by the calcium acetate diffused into

droplets and caused the sodium alginate to cross-link into calcium alginate hydrogel to form the stable core-shell particles (Fig. 5d). It was noteworthy that shrinkage of the beads would appear due to the cross-linking, so the diameter of the beads decreased about 40 % compared to the original droplets.

Generally, in microfluidic chips, microscale core-shell particles were usually synthesized using the coaxial devices (Agarwal et al. 2013; Kim et al. 2011; Rao et al. 2014; Shang et al. 2014; Windbergs et al. 2013). It was obvious that this coaxial structure needed specific micro-electromechanical system (MEMS) technique to fabricate. Otherwise, special needles were required which needed unique molds to fabricate and were only commercial available. These stratagems were not familiar in common labs. Moreover, all these coaxial structures or commercial needles had fixed character parameters, which could not be adjusted unless changing the needles or fabricating a new structure. It limited the versatile generation of different kinds of core-shell droplets. However, our nozzle was fabricated just using multilayer soft lithography, and

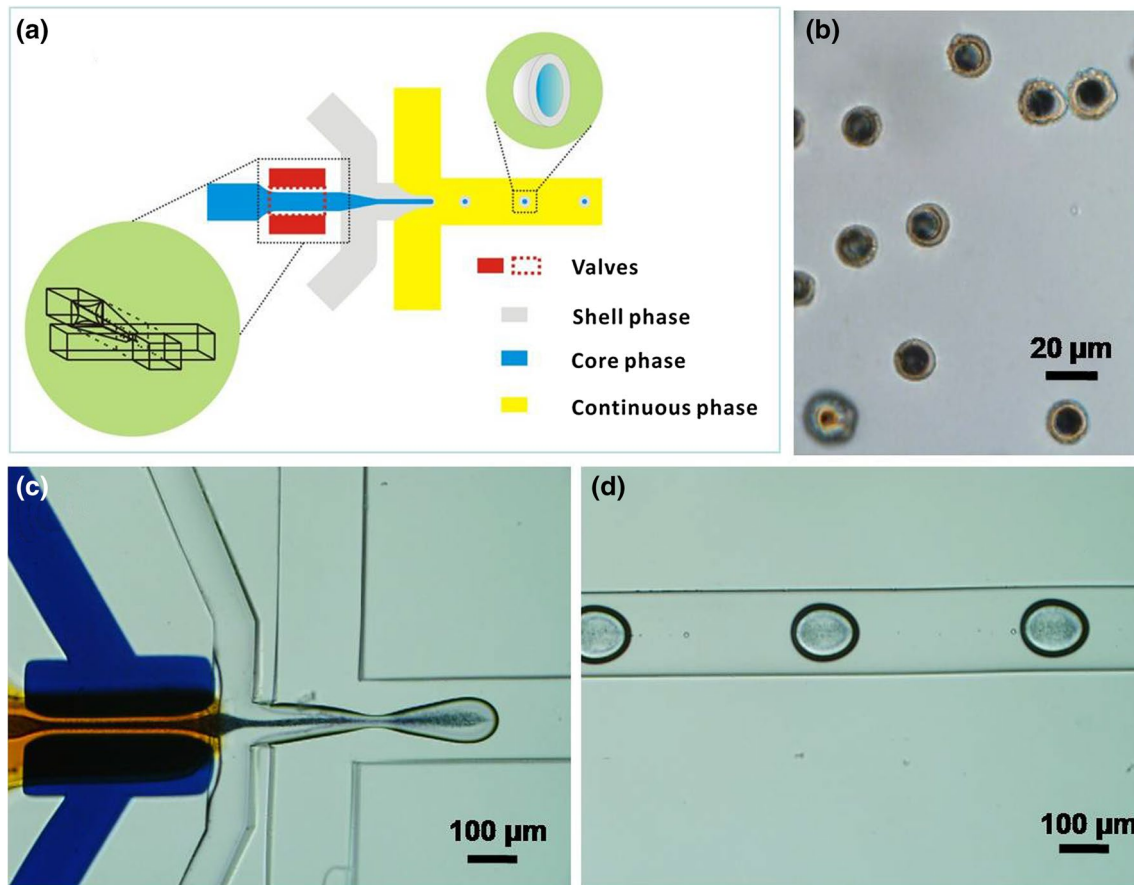


Fig. 5 **a** Schematics showing the core–shell microparticle formation when the 3D valve-based nozzle formed a specific structure. **b** Bright-field image of the generated calcium alginate core–shell particles in microscale. **c** 3D valve-based nozzle mounted on the multiplex flow-focusing structure for generating core–shell particles. **d**

Typical images showing gradual coverage process of the core fluid (1.5 % sodium alginate with Fe_3O_4 nanoparticles) by the shell fluid (1 % pure sodium alginate) and cross-linking of those droplets into hydrogel particles

this technique could be facily realized based on PDMS casting/bonding. And as the four fluid channel walls could be precisely controlled using our 3D nozzle, the shape of the nozzle could be adjusted, thus enabling versatile generation of core–shell particles. Compared to conventional microfluidic core–shell particle generation stratagems, our 3D valve-based nozzle was fabricated more easily and had better control and flexibility for the generation of smaller core–shell beads (less than $50\ \mu\text{m}$).

4 Conclusions

In conclusion, we designed a 3D controllable nozzle based on pneumatic valve structures. Utilizing the pressure modulation of the applied compressed air, the four walls of the fluid channel were precisely controlled to regulate the liquid flow inside. This actuator design had other unique functions such as microinjector or specific

nozzle. Compared to other pneumatic DOD regulation strategies, our 3D valve-based nozzle had advantages of faster response time and more precise and comprehensive control of droplet formation and composition. With appropriate control of the nozzle structure and fluid flow rates, our 3D valve-based nozzle enabled the generation of microscale core–shell particles, which was more facile and controllable than those commonly used coaxial needle molds. Our 3D valve-based nozzle provided a controllable, flexible and versatile droplet modulation strategy for those droplet-based assays that required fast, wide and effective control over the generation procedures, and it also offered a controllable platform for microscale core–shell particle synthesis. And due to the flexible control on individual orifice components of those flow-focusing regimes, our 3D nozzle also had potential applications for generating non-symmetrical particles when using hydrogel that could rapidly polymerize.

Acknowledgments This project was funded by the National Basic Research Program of China (Grant No. 2011CB933300), the National Science Fund for Talent Training in Basic Science (Grant No. J0830310), the National Natural Science Foundation of China (Grant Nos. 81402466 and 91433203) and the Fundamental Research Funds for the Central Universities (Grant No. 2015202020202).

References

- Abate AR, Romanowsky MB, Agresti JJ, Weitz DA (2009) Valve-based flow focusing for drop formation. *Appl Phys Lett* 94(2):023503
- Abate AR, Hung T, Mary P, Agresti JJ, Weitz DA (2010) High-throughput injection with microfluidics using picoinjectors. *Proc Natl Acad Sci USA* 107(45):19163–19166
- Agarwal P, Zhao S, Bielecki P, Rao W, Choi JK, Zhao Y, Yu J, Zhang W, He X (2013) One-step microfluidic generation of pre-hatching embryo-like core-shell microcapsules for miniaturized 3D culture of pluripotent stem cells. *Lab Chip* 13(23):4525–4533
- Angile FE, Vargo KB, Sehgal CM, Hammer DA, Lee D (2014) Recombinant protein-stabilized monodisperse microbubbles with tunable size using a valve-based microfluidic device. *Langmuir* 30(42):12610–12618
- Anna SL, Bontoux N, Stone HA (2003) Formation of dispersions using “flow focusing” in microchannels. *Appl Phys Lett* 82(3):364–366
- Baroud CN, Gallaire F, Dangla R (2010) Dynamics of microfluidic droplets. *Lab Chip* 10(16):2032–2045
- Cai B, Guo F, Zhao L, He R, Chen B, He Z, Yu X, Guo S, Xiong B, Liu W, Zhao X (2014) Disk-like hydrogel bead-based immunofluorescence staining toward identification and observation of circulating tumor cells. *Microfluid Nanofluid* 16(1–2):29–37
- Chen C-H, Miller MA, Sarkar A, Beste MT, Isaacson KB, Lauffenburger DA, Griffith LG, Han J (2013) Multiplexed protease activity assay for low-volume clinical samples using droplet-based microfluidics and its application to endometriosis. *J Am Chem Soc* 135(5):1645–1648
- Chiu DT, Lorenz RM, Jeffries GDM (2009) Droplets for ultrasmall-volume analysis. *Anal Chem* 81(13):5111–5118
- Chokkalingam V, Tel J, Wimmers F, Liu X, Semenov S, Thiele J, Figdor CG, Huck WTS (2013) Probing cellular heterogeneity in cytokine-secreting immune cells using droplet-based microfluidics. *Lab Chip* 13(24):4740–4744
- Chong ZZ, Tan SH, Ganan-Calvo AM, Tor SB, Loh NH, Nguyen N-T (2016) Active droplet generation in microfluidics. *Lab Chip* 16(1):35–58
- Christopher GF, Anna SL (2007) Microfluidic methods for generating continuous droplet streams. *J Phys D Appl Phys* 40(19):R319
- Collins DJ, Neild A, deMello A, Liu A-Q, Ai Y (2015) The Poisson distribution and beyond: methods for microfluidic droplet production and single cell encapsulation. *Lab Chip* 15(17):3439–3459
- Datta SS, Abbaspourrad A, Amstad E, Fan J, Kim S-H, Romanowsky M, Shum HC, Sun B, Utada AS, Windbergs M, Zhou S, Weitz DA (2014) 25th anniversary article: double emulsion templated solid microcapsules: mechanics and controlled release. *Adv Mater* 26(14):2205–2218
- Fu TT, Wu YN, Ma YG, Li HZ (2012) Droplet formation and breakup dynamics in microfluidic flow-focusing devices: from dripping to jetting. *Chem Eng Sci* 84:207–217
- Garrait G, Beyssac E, Subirade M (2014) Development of a novel drug delivery system: chitosan nanoparticles entrapped in alginate microparticles. *J Microencapsul* 31(4):363–372
- Guo F, Liu K, Ji X-H, Ding H-J, Zhang M, Zeng Q, Liu W, Guo S-S, Zhao X-Z (2010) Valve-based microfluidic device for droplet on-demand operation and static assay. *Appl Phys Lett* 97(23):233701
- Guo Z-X, Zeng Q, Zhang M, Hong L-Y, Zhao Y-F, Liu W, Guo S-S, Zhao X-Z (2011) Valve-based microfluidic droplet micromixer and mercury (II) ion detection. *Sens Actuators A* 172(2):546–551
- Guo F, Lapsley MI, Nawaz AA, Zhao Y, Lin S-CS, Chen Y, Yang S, Zhao X-Z, Huang TJ (2012a) A droplet-based, optofluidic device for high-throughput, quantitative bioanalysis. *Anal Chem* 84(24):10745–10749
- Guo MT, Rotem A, Heyman JA, Weitz DA (2012b) Droplet microfluidics for high-throughput biological assays. *Lab Chip* 12(12):2146–2155
- Hazel J, Krutkramelis K, Mooney P, Tomschik M, Gerow K, Oakey J, Gatlin JC (2013) Changes in cytoplasmic volume are sufficient to drive spindle scaling. *Science* 342(6160):853–856
- Hsieh A-H, Pan P-H, Lee A (2009) Rapid label-free DNA analysis in picoliter microfluidic droplets using FRET probes. *Microfluid Nanofluid* 6(3):391–401
- Jarosz Daniel F, Brown Jessica CS, Walker Gordon A, Datta Manoshi S, Ung WL, Lancaster Alex K, Rotem A, Chang A, Newby Gregory A, Weitz David A, Bisson Linda F, Lindquist S (2014) Cross-kingdom chemical communication drives a heritable, mutually beneficial prion-based transformation of metabolism. *Cell* 158(5):1083–1093
- Ji X-H, Cheng W, Guo F, Liu W, Guo S-S, He Z-K, Zhao X-Z (2011) On-demand preparation of quantum dot-encoded microparticles using a droplet microfluidic system. *Lab Chip* 11(15):2561–2568
- Kelly BT, Baret J-C, Taly V, Griffiths AD (2007) Miniaturizing chemistry and biology in microdroplets. *Chem Commun* 18:1773–1788
- Kim C, Chung S, Kim YE, Lee KS, Lee SH, Oh KW, Kang JY (2011) Generation of core-shell microcapsules with three-dimensional focusing device for efficient formation of cell spheroid. *Lab Chip* 11(2):246–252
- Lai CW, Lin YH, Lee GB (2008) A microfluidic chip for formation and collection of emulsion droplets utilizing active pneumatic micro-choppers and micro-switches. *Biomed Microdevices* 10(5):749–756
- Lee C-Y, Lin Y-H, Lee G-B (2009) A droplet-based microfluidic system capable of droplet formation and manipulation. *Microfluid Nanofluid* 6(5):599–610
- Liu YF, Yobas L (2015) Microfluidic emulsification through a monolithic integrated glass micronozzle suspended inside a flow-focusing geometry. *Appl Phys Lett* 106(17):174101
- Ochs CJ, Abate AR (2015) Rapid modulation of droplet composition with pincer microvalves. *Lab Chip* 15(1):52–56
- Oh KW, Lee K, Ahn B, Furlani EP (2012) Design of pressure-driven microfluidic networks using electric circuit analogy. *Lab Chip* 12(3):515–545
- Oh CK, Lee SW, Jeong OC (2015) Fabrication of pneumatic valves with spherical dome-shape fluid chambers. *Microfluid Nanofluid* 19(5):1091–1099
- Puigmarti-Luis J (2014) Microfluidic platforms: a mainstream technology for the preparation of crystals. *Chem Soc Rev* 43(7):2253–2271
- Rao W, Zhao S, Yu J, Lu X, Zynger DL, He X (2014) Enhanced enrichment of prostate cancer stem-like cells with miniaturized 3D culture in liquid core-hydrogel shell microcapsules. *Biomaterials* 35(27):7762–7773
- Rao L, Cai B, Wang J, Meng Q, Ma C, He Z, Xu J, Huang Q, Li S, Cen Y, Guo S, Liu W, Zhao X-Z (2015) A microfluidic electrostatic separator based on pre-charged droplets. *Sensors Actuators B Chem* 210:328–335

- Rosenfeld L, Lin T, Derda R, Tang SY (2014) Review and analysis of performance metrics of droplet microfluidics systems. *Microfluid Nanofluid* 16(5):921–939
- Shang L, Cheng Y, Wang J, Ding H, Rong F, Zhao Y, Gu Z (2014) Double emulsions from a capillary array injection microfluidic device. *Lab Chip* 14(18):3489–3493
- Teh S-Y, Lin R, Hung L-H, Lee AP (2008) Droplet microfluidics. *Lab Chip* 8(2):198–220
- Theberge AB, Courtois F, Schaerli Y, Fischlechner M, Abell C, Holfelder F, Huck WTS (2010) Microdroplets in microfluidics: an evolving platform for discoveries in chemistry and biology. *Angew Chem Int Ed* 49(34):5846–5868
- Unger MA, Chou H-P, Thorsen T, Scherer A, Quake SR (2000) Monolithic microfabricated valves and pumps by multilayer soft lithography. *Science* 288(5463):113–116
- Velasco D, Tumarkin E, Kumacheva E (2012) Microfluidic encapsulation of cells in polymer microgels. *Small* 8(11):1633–1642
- Wang W, Yang C, Li CM (2009) On-demand microfluidic droplet trapping and fusion for on-chip static droplet assays. *Lab Chip* 9(11):1504–1506
- Windbergs M, Zhao Y, Heyman J, Weitz DA (2013) Biodegradable core-shell carriers for simultaneous encapsulation of synergistic actives. *J Am Chem Soc* 135(21):7933–7937
- Yang C-G, Xu Z-R, Wang J-H (2010) Manipulation of droplets in microfluidic systems. *TrAC Trends Anal Chem* 29(2):141–157
- Yang S, Guo F, Kiraly B, Mao X, Lu M, Leong KW, Huang TJ (2012) Microfluidic synthesis of multifunctional Janus particles for biomedical applications. *Lab Chip* 12(12):2097–2102
- Yu L, Chen MCW, Cheung KC (2010) Droplet-based microfluidic system for multicellular tumor spheroid formation and anticancer drug testing. *Lab Chip* 10(18):2424–2432
- Yu X, He R, Li S, Cai B, Zhao L, Liao L, Liu W, Zeng Q, Wang H, Guo S-S, Zhao X-Z (2013) Magneto-controllable capture and release of cancer cells by using a micropillar device decorated with graphite oxide-coated magnetic nanoparticles. *Small* 9(22):3895–3901
- Zeng S, Li B, Su Xo, Qin J, Lin B (2009) Microvalve-actuated precise control of individual droplets in microfluidic devices. *Lab Chip* 9(10):1340–1343
- Zhao Y, Cheng Y, Shang L, Wang J, Xie Z, Gu Z (2015) Microfluidic synthesis of barcode particles for multiplex assays. *Small* 11(2):151–174